DUCTILITY AND FRACTURE IN A SUPERPLASTIC ALLOY

T. G. Langdon and F. A. Mohamed*

INTRODUCTION

Superplastic deformation provides the possibility of a simple and inexpensive procedure for producing complex shapes through various thermoforming operations. A considerable interest in superplasticity has therefore developed over the last decade, although, almost without exception, this interest has centred on the flow characteristics rather than the fracture behaviour per se. A series of detailed observations, primarily on various Cu-based alloys [1-3] but also on other materials such as microduplex steels [4,5], has now established that cavity formation is important in some superplastic alloys, but very little information is available on the factors which influence ductility in these materials. This paper describes results obtained from a program designed to investigate ductility and fracture characteristics in the Zn-22% Al eutectoid.

EXPERIMENTAL PROCEDURE

Experiments were performed on specimens of the Zn-22% Al eutectoid alloy having average equiaxed spatial grain diameters (defined as $1.74 \times \bar{L}$ where $\bar{L}$ is the mean linear intercept) in the range from 2.1 to 7.5 μm. Specimens were tested at constant temperatures from 403 ± 1 to 503 ± 1 K, by immersing in an electrically-heated silicone oil bath stirred with bubbling argon.

Two different specimen configurations were used in these experiments. For measurements of ductility, specimens were pulled in tension at a constant rate of cross-head displacement on an Instron testing machine. The specimen gauge length was set equal to 0.635 cm, so that high elongations could be achieved with the specimen fully submerged in the oil bath. For measurements of flow characteristics, specimens were tested either in tension or by using a double shear configuration [6].

DEPENDENCE OF DUCTILITY ON STRAIN RATE AND TEMPERATURE

Figure 1 shows typical results obtained for specimens having an initial grain size, d, of 2.5 μm, tested at temperatures, T, from 423 to 503 K. Each point represents a different specimen, and the data are plotted as $\Delta L/L_o$ % versus $\dot{\varepsilon}$, where ΔL is the total increase in length at the point of fracture, L_o is the initial specimen gauge length, and $\dot{\varepsilon}$ is the initial strain rate calculated from L_o.

*Department of Materials Science, University of Southern California, Los Angeles, California 90007, U.S.A.

The results reveal a number of interesting trends. First, maximum ductility occurs over an intermediate range of strain rate, and there is a decrease in the strain to failure at both very high and very low values of the imposed strain rate. It was demonstrated earlier that maximum ductility occurs when the strain rate sensitivity, m, is a maximum [7], where m is defined as the slope of a logarithmic plot of maximum flow stress, σ, versus strain rate, $\dot{\varepsilon}$. A review of the stress: strain rate data for the specimens utilized for the construction of Figure 1 shows that the same trend applies, since $m \sim 0.22$ at low $\dot{\varepsilon}$ (region I), increases to ~ 0.5 at intermediate $\dot{\varepsilon}$ (region II), and then decreases again at high $\dot{\varepsilon}$ (region III) [8]. Second, the peak ductility occurs at higher strain rates as the temperature is increased. Third, the magnitude of the maximum attainable ductility increases with increasing temperature. The result of these trends is that maximum ductility occurs at the highest temperature at high and intermediate strain rates, but at the lowest temperature at very low strain rates.

The macroscopic fracture characteristics may be appreciated from an examination of the specimens at fracture, as shown in Figure 2: specimens A are untested, and specimens B to J were pulled to failure over decreasing strain rates covering five orders of magnitude, from 1.33 to 1.33×10^{-5} s^{-1}, respectively. Figure 2(a) shows the specimens tested at 503 K, where the fastest strain rate yielded a fracture strain of $\sim$430% (specimen B), a maximum elongation of $\sim$2850% was observed at 1.33×10^{-2} s^{-1} (specimen F), and the fracture strain was reduced to $\sim$400% at the lowest strain rate (specimen J). The appearance of these specimens at the macroscopic level indicates two distinct types of failure: (i) necking occurs at high and low strain rates, (ii) the specimens pull out to a fine point and the behaviour is superplastic at intermediate strain rates.

A similar sequence is visible in Figure 2(b) for the specimens tested at 423 K, although in this case the maximum attainable ductilities were much lower. There is also evidence at this temperature for a third type of fracture at the fastest strain rate (specimen B), where the specimen broke in a quasi-brittle manner with little or no necking, and an overall ductility of only $\sim$70%. The occurrence of two necks within the gauge length is clearly visible at the lowest strain rate (specimen J).

The approximate ranges of strain rate for these three macroscopic types of failure (quasi-brittle, necking, and superplastic) are indicated in Figure 1 for a temperature of 423 K.

INTERPRETATION OF THE DUCTILITY RESULTS

The results presented in Figure 1 show that the strain at failure in a superplastic alloy depends critically on the testing temperature and imposed strain rate. No detailed theory is at present available which accurately predicts the variation of ductility with external variables. However, an analysis may be performed by considering the dependence of ductility on the strain rate sensitivity and temperature.

In a qualitative sense, the ductility data show that high strains at failure, in excess of 2000% for Zn-22% Al, are associated with a high strain rate sensitivity ($m \sim 0.5$) at intermediate strain rates. Any definitive analysis is difficult because the total extension achieved in tension is composed of two components having no sharp demarcation: a

uniform extension up to the point of necking, and a localized extension after necking.

According to the model for plastic instability developed by Hart [9], the condition for stable and uniform deformation is

$$(\kappa/\varepsilon) + m \geq 1 \tag{1}$$

where κ is the coefficient of strain hardening and ε is the true strain. Thus, for a constant value of κ,

$$\varepsilon = f(1-m)^{-1} \tag{2}$$

The true strain is defined as

$$\varepsilon = \ell n\ (L/L_o) = \ell n\ (1 + \Delta L/L_o) \tag{3}$$

where L is the instantaneous length. Since $\Delta L/L_o \gg 1$ for superplastic behaviour, equations (2) and (3) lead to

$$(\Delta L/L_o)_f = C(T,d,\ldots)\ \exp\ (C'/[1-m]) \tag{4}$$

where C includes the functional dependence on external variables such as temperature and grain size, C' is a constant, and the subscript f denotes the assumption that $(\Delta L/L_o)$ at the onset of non-uniform deformation is directly proportional to $(\Delta L/L_o)_f$ at fracture.

It is generally observed at elevated temperatures that ductility increases with increasing temperature [10]. Since the rate of plastic flow depends on the activation energy for the rate-controlling process, Q, it seems reasonable, as a first approximation, to relate ductility to temperature through a linear function of the form f(RT/Q), where R is the gas constant. Equation (4) therefore becomes

$$(\Delta L/L_o)_f = C''(RT/Q)\ \exp\ (C'/[1-m]) \tag{5}$$

where C'' is a constant under conditions of constant grain size.

The validity of this analysis was tested by the following procedure:

i) It was assumed that the superplastic region II and the low strain rate region I arise through the sequential operation of two different processes, and these combine independently with the high strain rate region III [11]. The average value of m appropriate to any strain rate was then calculated using standard procedures for sequential and independent processes [12].

ii) The values of C' and C'' at 473 K were estimated from the ductility curve shown in Figure 1 by setting $\Delta L/L_o = 4$ and $Q = 119$ kJ mol^{-1} [11] at the lowest value of m in region I, and $\Delta L/L_o = 28$ and $Q = 78.8$ kJ mol^{-1} [11] at the highest value of m in region II. These two points are designated A and B in Figure 3, and the values obtained for C' and C'' were 6.9 and 1.2×10^{-2}, respectively.

The predicted variation of $\Delta L/L_o$ with $\dot{\varepsilon}$ at 473 K is shown by the solid line in Figure 3, and the corresponding prediction at 423 K, using the same values for the constants C' and C'', is given by the lower broken curve. These two curves are generally similar in appearance to the experimental results shown in Figure 1. Specifically: (i) the peak in the curve at 423 K is shifted to a lower strain rate, and (ii) the ratio of the maximum ductilities at the peaks of the curves is predicted as $\sim$1.64, which compares very favourably with the experimental ratio of $\sim$1.69.

DUCTILITY MAPS

There has been considerable recent interest in the possibility of presenting mechanical data in the form of deformation mechanism maps, and maps are now available for several materials including two superplastic alloys [13]. Figure 4 shows an example of a deformation mechanism map for Zn-22% Al at a temperature of 473 K, plotted in the form of normalized grain size, d/b, versus normalized shear stress, τ/G, where b is the Burgers vector and G is the shear modulus. This map shows the superplastic region II, together with the less superplastic regions I and III and the regions associated with Nabarro-Herring and Coble diffusional creep.

The extensive ductility results now available from this program, especially in regions I and II, permit the construction of a ductility map of the type shown in Figure 5. The contours at low d/b and high τ/G are based on experimental measurements, and indicate very clearly the variation in total ductility with stress and grain size. Insufficient results are available in region III and at very low stress levels to provide contours over the entire map. However, it is reasonable to assume that ductility decreases at large grain sizes and high stresses, ultimately giving brittle failure. The situation at very low stresses is less clear, since the occurrence of Newtonian viscous diffusional processes, with m = 1, suggests the possibility of extremely high ductilities. Unfortunately, the strain rates involved under these conditions are very low, and it is difficult to perform laboratory experiments to measure ductility in this region.

SUMMARY AND CONCLUSIONS

The ductility observed in the superplastic Zn-22% Al eutectoid alloy depends critically on the testing temperature and the imposed strain rate. It is shown that results obtained at temperatures from 423 to 503 K may be explained by considering the dependence of ductility on the strain rate sensitivity and temperature. A ductility map is introduced, which plots, at constant temperature, contours of constant fracture strain on a field of grain size versus stress.

ACKNOWLEDGEMENT

This work was supported by the National Science Foundation under Grant No. DMR72-03238 A01.

REFERENCES

1. DUNLOP, G. L., SHAPIRO, E., TAPLIN, D. M. R. and CRANE, J., Met. Trans., 4, 1973, 2039.
2. FLECK, R. G., BEEVERS, C. J. and TAPLIN, D. M. R., J. Mater. Sci., 9, 1974, 1737.
3. SAGAT, S. and TAPLIN, D. M. R., Acta Met., 24, 1976, 307.
4. HUMPHRIES, C. W. and RIDLEY, N., J. Mater. Sci., 9, 1974, 1429.
5. SMITH, C. I., NORGATE, B. and RIDLEY, N., Met. Sci., 10, 1976, 182.
6. MOHAMED, F. A. and LANGDON, T. G., Acta Met., 23, 1975, 117.
7. ISHIKAWA, H., MOHAMED, F. A. and LANGDON, T. G., Phil. Mag., 32, 1975, 1269.
8. MOHAMED, F. A., AHMED, M. M. I. and LANGDON, T. G., Met. Trans. (submitted for publication).
9. HART, E. W., Acta Met., 15, 1967, 351.
10. DIETER, G. E., Ductility, ASM, Metals Park, Ohio, 1968, 1.
11. MOHAMED, F. A., SHEI, S.-A. and LANGDON, T. G., Acta Met., 23, 1975, 1443.
12. LANGDON, T. G. and MOHAMED, F. A., to be published.
13. MOHAMED, F. A. and LANGDON, T. G., Scripta Met., 10, 1976, 759.

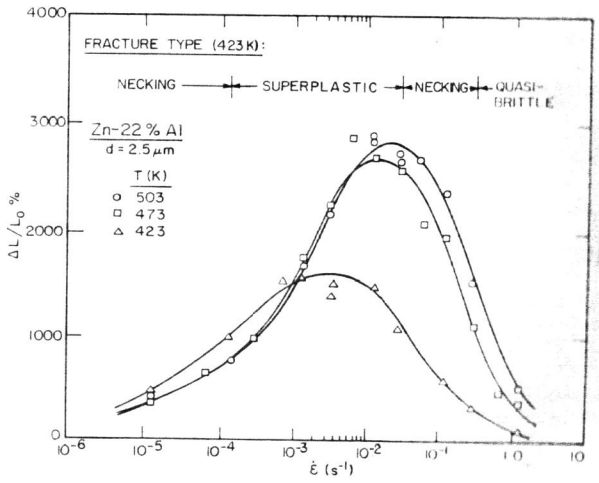

Figure 1 Tensile Fracture Strain Versus Initial Strain Rate: The Fracture Types at 423 K are Indicated

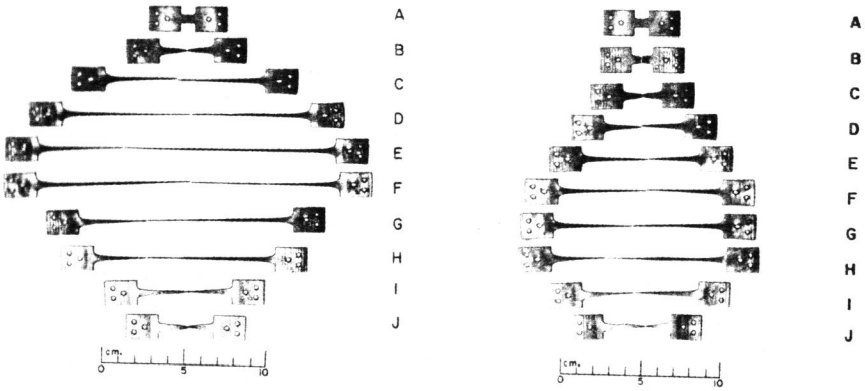

Figure 2 Specimen A is Untested. The Other Specimens were Tested to Failure at Initial Strain Rates from 1.33 s^{-1} (Specimen B) to 1.33 x 10^{-5} s^{-1} (Specimen J) at (a) 503 K, (b) 423 K

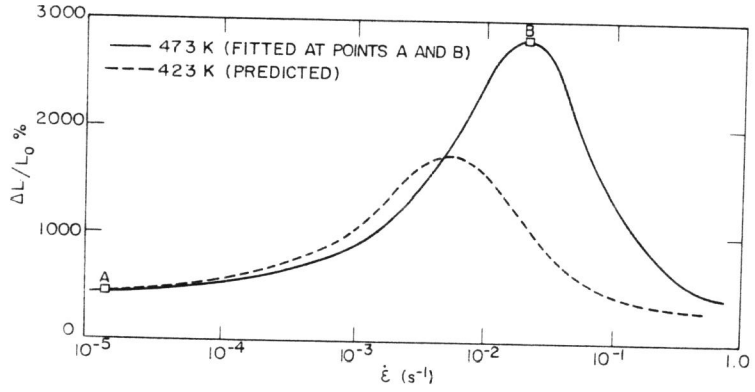

Figure 3 Predicted Variation of Fracture Strain with Initial Strain Rate at 473 and 423 K, with the Line for 473 K Fitted to the Experimental Data at Points A and B

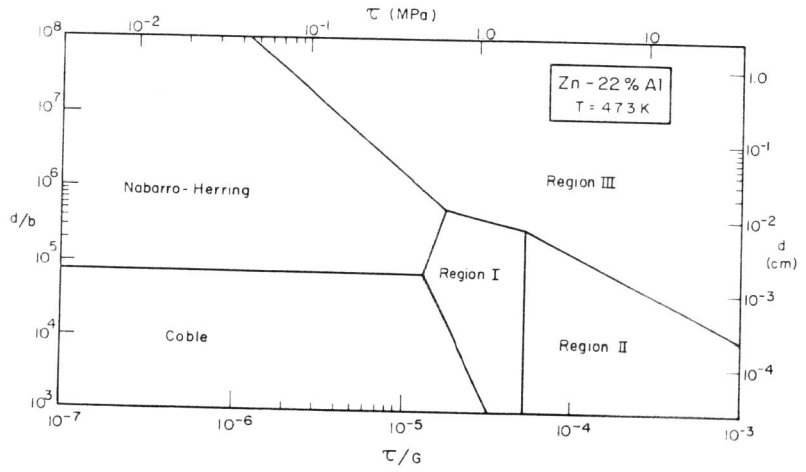

Figure 4 Deformation Mechanism Map for Zn-22% Al at 473 K

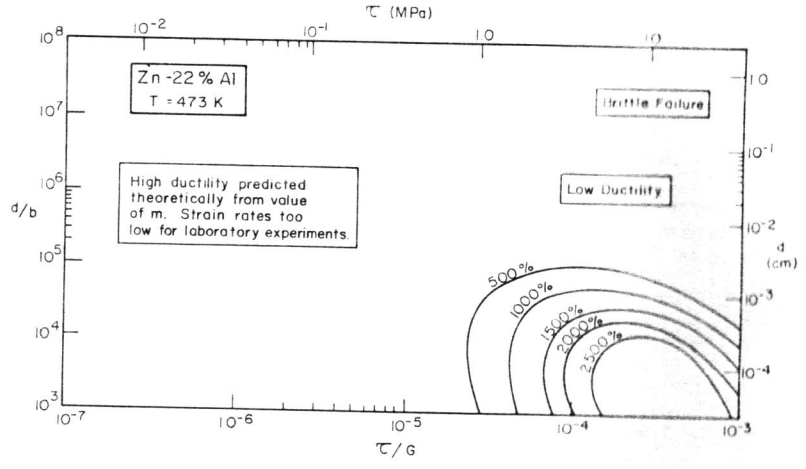

Figure 5 Ductility Map for Zn-22% Al at 473 K